

Impact of graphene coating on the atom-plate interaction

G. L. Klimchitskaya^{1,2} and V. M. Mostepanenko^{1,2}

¹*Central Astronomical Observatory at Pulkovo of the
Russian Academy of Sciences, St.Petersburg, 196140, Russia*

²*Institute of Physics, Nanotechnology and Telecommunications,
St.Petersburg State Polytechnical University, St.Petersburg, 195251, Russia*

Abstract

Using the recently proposed quantum electrodynamical formalism, we calculate the Casimir-Polder free energies and forces between the ground state atoms of Rb, Na, Cs and He* and the plates made of Au, Si, sapphire and fused silica coated with a graphene sheet. It is shown that the graphene coating has no effect on the Casimir-Polder interaction for metallic plates, but influences significantly for plates made of dielectric materials. The influence of graphene coating increases with decreasing static dielectric permittivity of the plate material and the characteristic frequency of an atomic dynamic polarizability. Simple analytic expressions for the classical limit of the Casimir-Polder free energy and force between an atom and a graphene-coated plate are obtained. From the comparison with the results of numerical computations, the application region of these expressions is determined.

PACS numbers: 34.35.+a, 12.20.Ds, 78.67.Wj

I. INTRODUCTION

The interaction of a polarizable atom in the ground state with an ideal metal plate at zero temperature, caused by the zero-point oscillations of the electromagnetic field, was described by Casimir and Polder [1]. It was generalized to the plate materials characterized by the frequency-dependent dielectric permittivity $\varepsilon(\omega)$ at nonzero temperature in the framework of the Lifshitz theory [2]. In succeeding years much work has been done to investigate the dependence of the Casimir-Polder interaction on the characteristics of atoms and properties of plate materials [3–8]. These theoretical investigations were stimulated by the experimental studies of quantum reflection [9–11] and Bose-Einstein condensation [12–14] of different atoms near material surfaces. Furthermore, after a qualitative experimental demonstration of the atom-plate interaction [15], more precise measurement of the thermal Casimir-Polder force has been performed [16] using the advantages of Bose-Einstein condensation. The results of this measurement were used to obtain stronger constraints on the Yukawa-type corrections to Newtonian gravitational law [17] and on the coupling constants of axion-like particles [18].

After the discovery of graphene, which is a two-dimensional sheet of carbon atoms, much theoretical attention was given to the interaction of atoms with this unusual material. These investigations became quantitative with the development of the Dirac model of graphene which assumes the linear dispersion relation for the graphene bands at low energies [19, 20]. First, the Dirac model was used to find the reflection properties of electromagnetic oscillations on graphene and calculate the van der Waals and Casimir interaction between two graphene sheets and between a graphene sheet and a material plate [21–29]. Next, the Casimir-Polder interaction of different atoms with graphene has been calculated [30–34]. This was done by effectively expressing the reflection properties of graphene either in terms of the density-density correlation functions [22, 25, 26, 33] or via the components of the polarization tensor in (2+1)-dimensional space-time [21, 24, 27–29, 32, 34]. In so doing, it was discovered that the thermal effect in the Casimir and Casimir-Polder interactions with graphene sheet becomes relatively large at much shorter separations than for usual materials [22, 24, 25, 27–29, 32, 34].

Until the present time, the Casimir-Polder interaction between atoms and a graphene sheet has not been measured. This is a complicated problem bearing in mind that it would

be difficult to preserve the flatness of a freestanding graphene under the influence of force on the source side of atoms. The pioneer measurement of the Casimir force in graphene research was performed in the configuration of an Au sphere and a graphene sheet deposited on a SiO₂ film covering a Si plate [35]. The comparison of the experimental data with the Lifshitz theory required knowledge of the reflection coefficients of electromagnetic fluctuations on graphene-coated substrates. Coefficients of this kind were found in Refs. [25, 36, 37], but expressed via the longitudinal and transverse density-density correlation functions (or, equivalently, respective electric susceptibilities) of graphene. However, only the longitudinal correlation function was explicitly known and only at zero temperature, and this made precise calculations hard. The situation has been changed after the publication of Ref. [38] where both the longitudinal and transverse density-density correlation functions were found at any nonzero temperature by expressing them via the explicitly known components of the polarization tensor. Simultaneously with this, the reflection coefficients on graphene-coated substrates were immediately expressed via the components of the polarization tensor of graphene and the dielectric permittivity of a substrate [39]. When compared with the measurement data of the experiment [35], the Lifshitz theory using these reflection coefficients has led to a very good agreement [39]. This opened up opportunities to the investigation of the Casimir-Polder interaction between different atoms and graphene-coated plates.

In this paper, we use the recently proposed formalism of Ref. [39] to calculate the Casimir-Polder free energies and forces between different atoms and graphene-coated plates made of different materials. We consider the atoms of Rb, Na, Cs and He* (metastable helium) and the plates made of Au, Si, sapphire (Al₂O₃) and fused silica (SiO₂) coated with a graphene sheet. We determine the influence of graphene coating on the Casimir-Polder free energy and force at room temperature. According to our results, graphene coating of metallic plates has no effect on the atom-plate interaction. For dielectric plates the impact of graphene coating is the greater, the smaller is the static dielectric permittivity of plate material. We show that the impact of graphene coating on the Casimir-Polder interaction for a dielectric plate increases with decreasing characteristic frequency of the atomic dynamic polarizability. We also find the classical limit for the Casimir-Polder force between atoms and graphene-coated plates. The main terms in this limit do not depend on the plate material, in contrast to the case of uncoated plates.

The paper is organized as follows. In Sec. II we briefly describe the formalism of the

Lifshitz theory adapted to calculate the Casimir-Polder interaction between atoms and graphene-coated plates. Then the computational results for the influence of graphene on the free energy are presented. In Sec. III the influence of graphene coating on the Casimir-Polder force is investigated and the classical (high-temperature) limit is derived. Section IV contains our conclusions and discussion.

II. FREE ENERGY OF ATOMS INTERACTING WITH GRAPHENE-COATED PLATES

Here, we introduce the used formalism, specifically, the reflection coefficients of the electromagnetic fluctuations on a graphene-coated plate, where graphene is described by the polarization tensor, and the plate material by the frequency-dependent dielectric permittivity. Then we calculate the free energy of the Casimir-Polder interaction between different atoms and graphene-coated plates made of various materials and determine the influence of graphene coating.

A. Formalism and notations

We consider a ground state atom described by the atomic dynamic polarizability $\alpha(\omega)$ at a separation a from the plane plate described by the frequency-dependent dielectric permittivity $\varepsilon(\omega)$ coated with a graphene sheet. It is assumed that the plate is in thermal equilibrium with an environment at temperature T . The free energy of the Casimir-Polder interaction between an atom and a graphene-coated plate is given by the Lifshitz formula [2]. For the purpose of computations it is convenient to express it in terms of the dimensionless variables as follows [40]:

$$\begin{aligned} \mathcal{F}_g(a, T) = & -\frac{k_B T}{8a^3} \sum_{l=0}^{\infty}{}' \alpha(i\zeta_l \omega_c) \int_{\zeta_l}^{\infty} dy e^{-y} \\ & \times \{2y^2 R_{\text{TM}}(i\zeta_l, y) - \zeta_l^2 [R_{\text{TM}}(i\zeta_l, y) + R_{\text{TE}}(i\zeta_l, y)]\}. \end{aligned} \quad (1)$$

Here, k_B is the Boltzmann constant, the dimensionless Matsubara frequencies ζ_l are expressed via the dimensional ones by $\zeta_l \equiv \xi_l/\omega_c = 2a\xi_l/c$, where $\xi_l = 2\pi k_B T l/\hbar$ with $l = 0, 1, 2, \dots$, $\omega_c = c/(2a)$, and the prime on the summation sign indicates that the term with $l = 0$ is divided by two. The dimensionless variable y is connected with the

projection of the wave vector on the plane of plate, k_{\perp} , by the equation

$$y = 2a \left(k_{\perp}^2 + \frac{\xi_l^2}{c^2} \right)^{1/2}. \quad (2)$$

The reflection coefficients $R_{\text{TM,TE}}$ of the electromagnetic fluctuations on the graphene-coated plate for the transverse-electric (TE) and transverse-magnetic (TM) polarizations can be expressed via the dielectric permittivity of the plate material

$$\varepsilon_l \equiv \varepsilon^{(n)}(i\xi_l) = \varepsilon^{(n)}(i\zeta_l \omega_c), \quad (3)$$

and the dimensionless polarization tensor of graphene in (2+1)-dimensional space-time, $\tilde{\Pi}_{kn}$ ($k, n = 0, 1, 2$), connected with the dimensional one, Π_{kn} , by the equation

$$\tilde{\Pi}_{kn} \equiv \tilde{\Pi}_{kn}(i\zeta_l, y) = \frac{2a}{\hbar} \Pi_{kn}. \quad (4)$$

The explicit expressions for these reflection coefficients follow from the results of Refs. [26, 36, 37] if to take into account the relationship between the density-density correlation function and the polarization tensor found in Ref. [38]. Alternatively, the same expressions were immediately obtained in Ref. [39] by other means. They are given by [39]

$$R_{\text{TM}}(i\zeta_l, y) = \frac{\varepsilon_l y + k_l \left(\frac{y}{y^2 - \zeta_l^2} \tilde{\Pi}_{00} - 1 \right)}{\varepsilon_l y + k_l \left(\frac{y}{y^2 - \zeta_l^2} \tilde{\Pi}_{00} + 1 \right)}, \quad (5)$$

$$R_{\text{TE}}(i\zeta_l, y) = \frac{y - k_l - \left(\tilde{\Pi}_{\text{tr}} - \frac{y^2}{y^2 - \zeta_l^2} \tilde{\Pi}_{00} \right)}{y + k_l + \left(\tilde{\Pi}_{\text{tr}} - \frac{y^2}{y^2 - \zeta_l^2} \tilde{\Pi}_{00} \right)},$$

where $\tilde{\Pi}_{\text{tr}}$ is the sum of the spatial components $\tilde{\Pi}_1^1$ and $\tilde{\Pi}_2^2$, and the following notation is introduced

$$k_l \equiv \sqrt{y^2 + (\varepsilon_l - 1)\zeta_l^2}. \quad (6)$$

The computations below require analytic expressions for the quantities $\tilde{\Pi}_{00}$ and $\tilde{\Pi}_{\text{tr}}$. These quantities depend on T both explicitly, as on a parameter, and implicitly through the Matsubara frequencies. It was shown [24, 27, 28, 32] that an explicit dependence on T influences the computational results for the free energy and force only through the zero-frequency term of the Lifshitz formula $l = 0$. In the region of separations considered below ($a \geq 100$ nm) all terms of Eq. (1) with $l \geq 1$ without the loss of accuracy can be calculated

using the simplified polarization tensor defined at $T = 0$ and depending on T only implicitly through the Matsubara frequencies.

We consider undoped gapless graphene (as shown in Ref. [32], at $T = 300$ K the influence of nonzero gap below 0.1 eV on the computational results is negligibly small). Under these conditions, at $\zeta_0 = 0$ the exact expressions for the temperature-dependent components of the polarization tensor in Eq. (5) are the following [24, 27, 32]:

$$\begin{aligned}\tilde{\Pi}_{00}(0, y) &= \frac{8\alpha\tau}{\pi\tilde{v}_F^2} \int_0^1 dx \ln \left(2 \cosh \frac{\pi\theta}{\tau} \right), \\ \tilde{\Pi}_{\text{tr}}(0, y) - \tilde{\Pi}_{00}(0, y) &= 8\alpha\tilde{v}_F^2 y^2 \int_0^1 dx \frac{x(1-x)}{\theta} \tanh \frac{\pi\theta}{\tau}.\end{aligned}\tag{7}$$

Here, $\alpha = e^2/(\hbar c)$ is the fine-structure constant, the dimensionless temperature parameter τ is defined as $\tau \equiv 4\pi a k_B T/(\hbar c)$, $\tilde{v}_F = v_F/c$, where $v_F \approx 9 \times 10^5$ m/s is the Fermi velocity in graphene [41, 42], and the function θ is given by

$$\theta \equiv \theta(x, y) = \tilde{v}_F y \sqrt{x(1-x)}.\tag{8}$$

As explained above, at all Matsubara frequencies ζ_l with $l \geq 1$ we can use the following components of the polarization tensor found in Ref. [21] at $T = 0$, where the continuous parameter ζ is replaced with the discrete ζ_l :

$$\begin{aligned}\tilde{\Pi}_{00}(i\zeta_l, y) &= \pi\alpha \frac{y^2 - \zeta_l^2}{f(\zeta_l, y)}, \\ \tilde{\Pi}_{\text{tr}}(i\zeta_l, y) - \frac{y^2}{y^2 - \zeta_l^2} \tilde{\Pi}_{00}(i\zeta_l, y) &= \pi\alpha f(\zeta_l, y),\end{aligned}\tag{9}$$

where the function f is defined as

$$f(\zeta_l, y) = [\tilde{v}_F^2 y^2 + (1 - \tilde{v}_F^2) \zeta_l^2]^{1/2}.\tag{10}$$

As a result, the free energy of the Casimir-Polder interaction between an atom and a material plate coated with graphene can be calculated using Eqs. (1) and (5) supplemented by Eqs. (6)–(10).

B. Influence of graphene on the free energy

To find the influence of the graphene coating on the Casimir-Polder free energy, we calculate the free energies of atom-plate interaction in the absence, \mathcal{F} , and in the presence,

\mathcal{F}_g , of graphene coating [in the former case the polarization operator in Eq. (5) should be put equal to zero]. We begin with an atom of Rb interacting with the plates made of Au, Si, sapphire (Al_2O_3), and fused silica (SiO_2). At separations above 100 nm considered here one can describe the atomic dynamic polarizability with sufficient precision using the single-oscillator model [3, 6]

$$\alpha(i\xi_l) = \frac{\alpha(0)}{1 + \frac{\xi_l^2}{\omega_0^2}}, \quad (11)$$

where $\alpha(0)$ is the static polarizability and ω_0 is the characteristic frequency. For the atom of Rb one has $\alpha(0) = 319.9$ a.u. and $\omega_0 = 5.46$ eV (note that 1 a.u. of polarizability is equal to 1.482×10^{-31} m³).

To perform computations using Eqs. (1) and (5), one also needs the dielectric permittivities of plate materials ε_l computed at the imaginary Matsubara frequencies. For Au the values of ε_l were obtained by means of the Kramers-Kronig relation from the tabulated optical data [44] extrapolated down to zero frequency [40, 45]. Note that for the atom-plate interaction the computational results for the free energy and force do not depend on the type of extrapolation of the optical data by means of the Drude or the plasma model [40, 45] (the values of the plasma frequency $\omega_p = 9$ eV and the relaxation parameter $\gamma = 0.035$ eV have been used in extrapolations). For high-resistivity Si the values of ε_l were obtained with the help of the Kramers-Kronig relation from the tabulated data [46]. As to other dielectric materials (sapphire and fused silica), we have used sufficiently precise analytic representations for their frequency-dependent dielectric permittivities [47].

In Fig. 1, the ratios of the Casimir-Polder free energies $\mathcal{F}_g/\mathcal{F}$ computed for the interaction of a Rb atom with Au, Si, Al_2O_3 and SiO_2 plates at $T = 300$ K are shown by the four solid lines as functions of separation. As can be seen in this figure, there is no influence of graphene coating on the Casimir-Polder interaction of Rb atom with an Au plate. The same holds for any atom interacting with any plate made of a metal or metallic-type semiconductor. At the same time, according to Fig. 1, there is considerable influence of graphene coating on the interaction free energy of a Rb atom with plates made of different dielectric materials. Thus, even at the shortest separation, $a = 100$ nm, the quantity $\mathcal{F}_g/\mathcal{F}$ takes the values 1.011, 1.038, and 1.10 for Si, Al_2O_3 and SiO_2 plates, respectively. At the separation of $a = 200$ nm the respective values of $\mathcal{F}_g/\mathcal{F}$ are equal to 1.015, 1.043, and 1.12, and at $a = 6$ μm achieve 1.19, 1.22, and 1.70, respectively. As is seen in Fig. 1, the influence of graphene coating on

the Casimir-Polder free energy increases with decreasing static dielectric permittivity of the plate material. The largest influence is obtained for a SiO₂ plate ($\epsilon_0 = 3.8$). The influence of graphene coating becomes weaker for Al₂O₃ and Si plates ($\epsilon_0 = 10.1$ and 11.7, respectively).

Large influence of graphene coating on the Casimir-Polder interaction in the case of dielectric plates is explained by the extraordinary large thermal effect inherent in this two-dimensional material. As an example, in Fig. 2(a) the ratios of the free energy at $T = 300$ K to the energy at $T = 0$ K for a Rb atom interacting with an uncoated (the line 1) and graphene-coated (the line 2) SiO₂ plate are presented as functions of separation. As is seen in this figure, for a graphene-coated plate the thermal effect is much more pronounced than for an uncoated one. This leads to a faster increase of the line 2, compared to the line 1, with the increase of separation (which is equivalent to the increase of temperature in calculations of the Casimir and Casimir-Polder forces [40]).

To explain the role of the thermal effect in more detail, in Fig. 2(b) we plot the ratios $\mathcal{F}_g/\mathcal{F}$ for the Casimir-Polder interactions with a graphene-coated and an uncoated SiO₂ plates as functions of separation at $T = 300$ K (the solid line) and at $T = 0$ K (the dashed line). Thus, the solid line reproduces the upper line in Fig. 1, whereas the dashed line represents the ratio of the Casimir-Polder energies, E_g/E , for a graphene-coated and uncoated SiO₂ plates. As can be seen in Fig. 2(b), large influence of graphene coating occurs only at $T = 300$ K. For the dashed line computed at $T = 0$ K one has $E_g/E = 1.07$ and 1.03 at $a = 100$ nm and $6 \mu\text{m}$, respectively, i.e., the role of graphene coating is limited to only a few percent.

Now we investigate the role of graphene coating of a plate interacting with different atoms. For this purpose we calculate the quantity $\mathcal{F}_g/\mathcal{F}$ as a function of separation for atoms of Rb, Na, Cs, and He* interacting with a SiO₂ plate (see the lines 1, 2, 3, and 4 in Fig. 3, respectively). Taking into account that the influence of atomic properties is more pronounced at the shortest separations, here we consider the separation region from 100 nm to $1 \mu\text{m}$. The atomic dynamic polarizabilities used in computations are given by Eq. (11). For an atom of Na the oscillator parameters are given by $\alpha(0) = 162.68$ a.u., $\omega_0 = 2.14$ eV [48]. For an atom of Cs one has $\alpha(0) = 403.6$ a.u., $\omega_0 = 1.55$ eV [48, 49], and for an atom of He* it holds $\alpha(0) = 315.638$ a.u., $\omega_0 = 1.18$ eV [50]. Note that the line 1 in Fig. 3 reproduces the initial part of the upper line in Fig. 1.

As is seen in Fig. 3, the influence of graphene coating on the free energy of the Casimir-Polder interaction increases with decreasing characteristic frequency. From Fig. 3 it follows

also that at the shortest separations considered the ratio $\mathcal{F}_g/\mathcal{F}$ becomes nonmonotonous (this is most appreciable for the Casimir-Polder interaction with an atom of He* marked by the maximum influence of graphene sheet). This corresponds to the regions of negative Casimir-Polder and Casimir entropy which were found in interactions of atoms with metallic plates [3] and between metallic and dielectric plates [51].

III. THE CASIMIR-POLDER FORCE

Although the Casimir-Polder free energy is the most important quantity for the experiments on quantum reflection [9–11], the major role in the experiments on Bose-Einstein condensation is played by the Casimir-Polder force. Here, we calculate this force for the case of graphene-coated plates, find the role of graphene, and obtain the analytic expressions for the classical limit which holds at large separations (high temperatures).

A. Influence of graphene coating on the force

In terms of dimensionless variables introduced in Sec. IIA the Casimir-Polder force between an atom and a graphene-coated plate is given by

$$F_g(a, T) = -\frac{k_B T}{8a^4} \sum_{l=0}^{\infty} \alpha(i\zeta_l \omega_c) \int_{\zeta_l}^{\infty} y dy e^{-y} \quad (12)$$

$$\times \{2y^2 R_{\text{TM}}(i\zeta_l, y) - \zeta_l^2 [R_{\text{TM}}(i\zeta_l, y) + R_{\text{TE}}(i\zeta_l, y)]\},$$

where the reflection coefficients $R_{\text{TM,TE}}$ are defined in Eq. (5).

To find the influence of graphene coating on the Casimir-Polder force we have computed the ratio F_g/F for the atom of He* at $T = 300$ K, where the index g indicates that the plate is coated with a graphene sheet. The computational results, as functions of separation, are presented in Fig. 4 by the four solid lines for Au, Si, Al₂O₃, and SiO₂ plates. Similar to the free energy, it is seen that the Casimir-Polder force between a He* atom and an Au plate is not influenced by the presence of graphene coating. For dielectric plates the influence of graphene coating increases with decreasing static dielectric permittivity of the plate material. These results remain valid for any one of metallic and dielectric plates. At short separation distances the influence of graphene on the Casimir-Polder force is slightly larger than on the free energy. Thus, at $a = 100$ nm, the quantity F_g/F takes the values

1.014, 1.051, and 1.145 for Si, Al₂O₃, and SiO₂ plates, respectively. At $a = 200 \text{ nm}$, the respective values of F_g/F are 1.018, 1.048, and 1.140, whereas at $a = 6 \mu\text{m}$ they are equal to 1.19, 1.22, and 1.70, i.e., the same as for the free energy.

Similar to the case of the free energy, large influence of graphene is explained by the extraordinary large thermal effect. This can be illustrated in close analogy to Fig. 2(a,b) presented above for the free energy. Similar to the free energy, for different atoms the influence of graphene coating on the Casimir-Polder force increases with decreasing characteristic frequency of the atomic dynamic polarizability, like it is shown in Fig. 3. Note that at short separations Fig. 4 demonstrates the nonmonotonous behavior which is explained by the same reason as was discussed in connection with Fig. 3.

B. High-temperature limit

In the limiting case of high temperatures (large separations) the main contribution to the Casimir-Polder and Casimir forces becomes classical. It is well investigated for atoms interacting with a graphene sheet [34], for two graphene sheets [28], and for a graphene sheet interacting with a material plate [27]. Here, we consider the classical limit for an atom interacting with a graphene-coated plate.

In the classical limit the total Casimir-Polder free energy and force are determined by the zero-frequency contribution to the Lifshitz formula, whereas all other terms are exponentially small [40]. Thus, from Eq. (1) we have

$$\mathcal{F}_g(a, T) = -\frac{k_B T}{8a^3} \alpha(0) \int_0^\infty y^2 dy e^{-y} R_{\text{TM}}(0, y). \quad (13)$$

For the TM reflection coefficient at zero frequency Eq. (5) leads to

$$\begin{aligned} R_{\text{TM}}(0, y) &= \frac{\varepsilon_0 y - y + \tilde{\Pi}_{00}(0, y)}{\varepsilon_0 y + y + \tilde{\Pi}_{00}(0, y)} \\ &= 1 - \frac{2y}{\tilde{\Pi}_{00}(0, y) + (\varepsilon_0 + 1)y}. \end{aligned} \quad (14)$$

In the case of metallic plates $\varepsilon_0 \rightarrow \infty$, $R_{\text{TM}}(0, y) \rightarrow 1$, and the classical limit (13) takes the trivial form

$$\mathcal{F}_g(a, T) = -\frac{k_B T}{4a^3} \alpha(0), \quad (15)$$

which does not depend on the presence of graphene coating in line with the above results. Below we consider a more rich case of dielectric plates where $\varepsilon_0 < \infty$.

We start from Eq. (7) and notice that in our region of parameters (we consider the fixed temperature $T = 300$ K and arbitrarily large separations $a \geq 100$ nm) it holds $\pi\theta/\tau \ll 1$. This is caused by the fact that the minimum value of τ achieved at $a = 100$ nm is equal to 0.164, and the main contribution to the integral (13) is given by $y \sim 1$. Then from Eq. (7) one obtains

$$\tilde{\Pi}_{00}(0, y) \equiv \tilde{\Pi}_{00}(0) \approx \frac{8\alpha}{\tilde{v}_F^2} \frac{\tau}{\pi} \ln 2 = 32\alpha \ln 2 \frac{ak_B Tc}{\hbar v_F^2}. \quad (16)$$

From Eq. (16) it follows that the quantity $\tilde{\Pi}_{00} \sim 10^3$ and it increases with the increase of separation. Thus, the first term in the denominator of Eq. (14) (the second line) is much larger than the second. Expanding the reflection coefficient R_{TM} in power of small parameter, we arrive at

$$R_{\text{TM}}(0, y) \approx 1 - \frac{2y}{\tilde{\Pi}_{00}(0)} + \frac{2(\varepsilon_0 + 1)}{\tilde{\Pi}_{00}^2(0)} y^2. \quad (17)$$

Substituting Eq. (17) in Eq. (13) and integrating with respect to y , we finally obtain

$$\begin{aligned} \mathcal{F}_g(a, T) \approx & -\frac{k_B T \alpha(0)}{4a^3} \left[1 - \frac{3\hbar v_F^2}{16\alpha \ln 2 ak_B Tc} \right. \\ & \left. + \frac{3(\varepsilon_0 + 1)\hbar^2 v_F^4}{128(\alpha \ln 2 ak_B Tc)^2} \right]. \end{aligned} \quad (18)$$

Note that the first two terms on the right-hand side of Eq. (18) coincide with the classical limit for the Casimir-Polder free energy of an atom interacting with a freestanding graphene sheet [34]. The third term on the right-hand side of Eq. (18) describes the role of a dielectric plate. This term is small in comparison with the first two. The main, classical, term in Eq. (18) is the same as for an atom interacting with metallic plate [see Eq. (15)].

Equation (18) should be compared with the classical Casimir-Polder free energy of an atom interacting with an uncoated dielectric plate [34]

$$\mathcal{F}(a, T) = -\frac{k_B T \alpha(0)}{4a^3} \frac{\varepsilon_0 - 1}{\varepsilon_0 + 1}. \quad (19)$$

It is seen that Eq. (19) more strongly depends on the static dielectric permittivity of plate material, as compared to Eq. (18).

Similar derivations can be performed for the classical limit of the Casimir-Polder force starting from Eq. (12). Alternatively, the classical limit for this force can be obtained by

the negative differentiation of Eq. (18) with respect to a with the following result:

$$F(a, T) \approx -\frac{3k_B T \alpha(0)}{4a^4} \left[1 - \frac{\hbar v_F^2}{4\alpha \ln 2ak_B T c} + \frac{5(\varepsilon_0 + 1)\hbar^2 v_F^4}{128(\alpha \ln 2ak_B T c)^2} \right]. \quad (20)$$

The first two terms on the right-hand side of Eq. (20) coincide with the Casimir-Polder force acting between an atom and a freestanding graphene sheet [34]. The influence of the dielectric plate is described by the third term depending on ε_0 . The respective Casimir-Polder force for an atom interacting with an uncoated dielectric plate is given by [34]

$$F(a, T) = -\frac{3k_B T \alpha(0)}{4a^4} \frac{\varepsilon_0 - 1}{\varepsilon_0 + 1}. \quad (21)$$

The right-hand side of this equation more strongly depends on ε_0 than the right-hand side of Eq. (20). For a graphene-coated metallic plate the classical Casimir-Polder force is the same as for an uncoated one

$$F_g(a, T) = F(a, T) = -\frac{3k_B T \alpha(0)}{4a^4}. \quad (22)$$

To determine the application region of Eqs. (20) and (22), we have performed numerical computations of the Casimir-Polder forces F_g at $T = 300$ K between an atom of He* and plates made of different materials coated with graphene sheet. The computational results for the quantity $|F_g|a^4$ as functions of separation are shown in Fig. 5 by the four solid lines from top to bottom for the plates made of Au, Si, Al₂O₃, and SiO₂, respectively. In an inset the region of large separations is shown in an enlarged scale. It can be seen that with increasing separation distance the Casimir-Polder force between an atom of metastable helium and graphene-coated plates made of different materials go to one and the same limit given by the first term in Eq. (20) and by Eq. (22).

We have compared the numerical results with the analytic ones calculated using Eq. (20) for dielectrics and Eq. (22) for metals. It was shown that for a graphene-coated SiO₂ plate (the smallest ε_0) Eq. (20) leads to the same force values, as the computed ones, in the limits of 2% error at all separations $a \geq 5 \mu\text{m}$. For Al₂O₃ and Si plates the coincidence between analytic and numerical results to within 2% occurs at $a \geq 5.5 \mu\text{m}$. As to the graphene-coated Au plate, the same measure of agreement between the two sets of results holds at $a \geq 6 \mu\text{m}$.

For comparison purposes in Fig. 6 we present the computational results for the quantity $|F|a^4$, where F is the Casimir-Polder force at $T = 300$ K between an atom of He* and

uncoated plates made of Au, Si, Al₂O₃, and SiO₂ (the solid line is for Au, and the dashed lines from top to bottom are for Si, Al₂O₃, and SiO₂, respectively). The comparison of Figs. 6 and 5 shows that the upper solid lines in both figures related to the Au plates coincide. This is in line with the above results stating that graphene coating on metallic plates does not influence the Casimir-Polder interaction. As to the dashed lines in Fig. 6 related to Si, Al₂O₃, and SiO₂ plates (from top to bottom), they are significantly different from the respective solid lines in Fig. 5. This is most pronounced with increasing separations where the lines in Fig. 6 go to the different limiting values prescribed by Eq. (22) for a metallic plate and by Eq. (21) for dielectric plates with different ϵ_0 .

The numerical results presented in Fig. 6 for an Au plate (the solid line) coincide in the limits of 2% error with the analytic ones of Eq. (22) at $a \geq 6 \mu\text{m}$. For uncoated dielectric plates the numerical results coincide with the analytic ones of Eq. (21) to within 2% starting from the same separations as for the plates coated with graphene (i.e., at $a \geq 5 \mu\text{m}$ for SiO₂ plate and at $a \geq 5.5 \mu\text{m}$ for Al₂O₃ and Si plates). One can conclude that although the graphene coating of dielectric plates significantly influences the Casimir-Polder interaction, it does not change the minimum separation distance starting with which the classical limit begins. This is different from the case of atom-graphene Casimir-Polder interaction where the classical limit occurs at $a \geq 1.5 \mu\text{m}$ [34], i.e., starting from by a factor of four shorter separations than for an atom interacting with an Au plate.

IV. CONCLUSIONS AND DISCUSSION

In this paper we have calculated the Casimir-Polder free energies and forces at $T = 300 \text{ K}$ between the ground state atoms of Rb, Na, Cs and He* and the plates made of Au, Si, sapphire and fused silica coated with a graphene sheet. The obtained results were compared with the free energies and forces for uncoated plates, and the influence of graphene coating was determined. It was found that the coating by graphene has no effect on the Casimir-Polder free energy and force in the case of metallic plates, but influences significantly for plates made of dielectric materials. The impact of graphene coating was shown to increase with decreasing static dielectric permittivity of the plate material and characteristic frequency of the atomic dynamic polarizability. Large influence of graphene coating on the Casimir-Polder free energy and force was explained by the extraordinary large thermal effect

discovered earlier in the van der Waals, Casimir and Casimir-Polder interactions with a graphene sheet.

In the foregoing we have also obtained simple analytic expressions for the classical limit of the Casimir-Polder free energy and force between atoms and graphene-coated plates. For metallic plates our result does not depend on the graphene coating, but for dielectric plates is influenced by the properties of graphene and (only slightly) by the static dielectric permittivity of the plate material. With increasing separation distance, the classical Casimir-Polder free energy and force go to the quantities which do not depend on the properties of graphene and material of the plate. This is different from the case of uncoated dielectric plates where the limiting values are material-dependent. We have compared the analytic expressions for the classical Casimir-Polder interaction with the results of numerical computations and determined the application region of the former.

The obtained results open prospective opportunities for using the graphene-coated samples in experiments on quantum reflection, Bose-Einstein condensation, and in various micro- and nanodevices.

-
- [1] H. B. G. Casimir and D. Polder, *Phys. Rev.* **73**, 360 (1948).
 - [2] E. M. Lifshitz and L. P. Pitaevskii, *Statistical Physics*, Pt.II (Pergamon Press, Oxford, 1980).
 - [3] J. F. Babb, G. L. Klimchitskaya, and V. M. Mostepanenko, *Phys. Rev. A* **70**, 042901 (2004).
 - [4] M. Antezza, L. P. Pitaevskii, and S. Stringari, *Phys. Rev. A* **70**, 053619 (2004).
 - [5] S. Y. Buhmann, L. Knöll, D.-G. Welsch, and H. T. Dung, *Phys. Rev. A* **70**, 052117 (2004).
 - [6] A. O. Caride, G. L. Klimchitskaya, V. M. Mostepanenko, and S. I. Zhanette, *Phys. Rev. A* **71**, 042901 (2005).
 - [7] S. Y. Buhmann and D.-G. Welsch, *Progr. Quant. Electronics* **31**, 51 (2007).
 - [8] V. B. Bezerra, G. L. Klimchitskaya, V. M. Mostepanenko, and C. Romero, *Phys. Rev. A* **78**, 042901 (2008).
 - [9] F. Shimizu, *Phys. Rev. Lett.* **86**, 987 (2001).
 - [10] H. Friedrich, G. Jacoby, and C. G. Meister, *Phys. Rev. A* **65**, 032902 (2002).
 - [11] V. Druzhinina and M. DeKieviet, *Phys. Rev. Lett.* **91**, 193202 (2003).
 - [12] D. M. Harber, J. M. McGuirk, J. M. Obrecht, and E. A. Cornell, *J. Low. Temp. Phys.* **133**,

- 229 (2003).
- [13] A. E. Leanhardt, Y. Shin, A. P. Chikkatur, D. Kielpinski, W. Ketterle, and D. E. Pritchard, *Phys. Rev. Lett.* **90**, 100404 (2003).
 - [14] Y.-j. Lin, I. Teper, C. Chin, and V. Vuletić, *Phys. Rev. Lett.* **92**, 050404 (2004).
 - [15] C. I. Sukenik, M. G. Boshier, D. Cho, V. Sandoghdar, and E. A. Hinds, *Phys. Rev. Lett.* **70**, 560 (1993).
 - [16] J. M. Obrecht, R. J. Wild, M. Antezza, L. P. Pitaevskii, S. Stringari, and E. A. Cornell, *Phys. Rev. Lett.* **98**, 063201 (2007).
 - [17] V. B. Bezerra, G. L. Klimchitskaya, V. M. Mostepanenko, and C. Romero, *Phys. Rev. D* **81**, 055003 (2010).
 - [18] V. B. Bezerra, G. L. Klimchitskaya, V. M. Mostepanenko, and C. Romero, *Phys. Rev. D* **89**, 035010 (2014).
 - [19] A. H. Castro Neto, F. Guinea, N. M. R. Peres, K. S. Novoselov, and A. K. Geim, *Rev. Mod. Phys.* **81**, 109 (2009).
 - [20] A. K. Geim, *Science* **324**, 1530 (2009).
 - [21] M. Bordag, I. V. Fialkovsky, D. M. Gitman, and D. V. Vassilevich, *Phys. Rev. B* **80**, 245406 (2009).
 - [22] G. Gómez-Santos, *Phys. Rev. B* **80**, 245424 (2009).
 - [23] D. Drosdoff and L. M. Woods, *Phys. Rev. A* **84**, 062501 (2011).
 - [24] I. V. Fialkovsky, V. N. Marachevsky, and D. V. Vassilevich, *Phys. Rev. B* **84**, 035446 (2011).
 - [25] V. Svetovoy, Z. Moktadir, M. Elvenspoek, and H. Mizuta, *Europhys. Lett.* **96**, 14006 (2011).
 - [26] Bo E. Sernelius, *Phys. Rev. B* **85**, 195427 (2012).
 - [27] M. Bordag, G. L. Klimchitskaya, and V. M. Mostepanenko, *Phys. Rev. B* **86**, 165429 (2012).
 - [28] G. L. Klimchitskaya and V. M. Mostepanenko, *Phys. Rev. B* **87**, 075439 (2013).
 - [29] G. L. Klimchitskaya and V. M. Mostepanenko, *Phys. Rev. B* **89**, 035407 (2014).
 - [30] Yu. V. Churkin, A. B. Fedortsov, G. L. Klimchitskaya, and V. A. Yurova, *Phys. Rev. B* **82**, 165433 (2010).
 - [31] T. E. Judd, R. G. Scott, A. M. Martin, B. Kaczmarek, and T. M. Fromhold, *New. J. Phys.* **13**, 083020 (2011).
 - [32] M. Chaichian, G. L. Klimchitskaya, V. M. Mostepanenko, and A. Tureanu, *Phys. Rev. A* **86**, 012515 (2012).

- [33] S. Ribeiro and S. Scheel, Phys. Rev. A **88**, 042519 (2013).
- [34] G. L. Klimchitskaya and V. M. Mostepanenko, Phys. Rev. A **89**, 012516 (2014).
- [35] A. A. Banishev, H. Wen, J. Xu, R. K. Kawakami, G. L. Klimchitskaya, V. M. Mostepanenko, and U. Mohideen, Phys. Rev. B **87**, 205433 (2013).
- [36] L. A. Falkovsky and S. S. Pershoguba, Phys. Rev. B **76**, 153410 (2007).
- [37] T. Stauber, N. M. R. Peres, and A. K. Geim, Phys. Rev. B **78**, 085432 (2008).
- [38] G. L. Klimchitskaya, V. M. Mostepanenko, and Bo E. Sernelius, Phys. Rev. B **89**, 125407 (2014).
- [39] G. L. Klimchitskaya, U. Mohideen, and V. M. Mostepanenko, Phys. Rev. B **89**, 115419 (2014).
- [40] M. Bordag, G. L. Klimchitskaya, U. Mohideen, and V. M. Mostepanenko, *Advances in the Casimir Effect* (Oxford University Press, Oxford, 2009).
- [41] B. Wunsch, T. Stauber, F. Sols, and F. Guinea, New J. Phys. **8**, 318 (2006).
- [42] N. M. R. Peres, F. Guinea, and A. H. Castro Neto, Phys. Rev. B **73**, 125411 (2006).
- [43] M. S. Safronova, C. J. Williams, and C. W. Clark, Phys. Rev. A **69**, 022509 (2004).
- [44] *Handbook of Optical Constants of Solids*, ed. E. D. Palik (Academic, New York, 1985).
- [45] G. L. Klimchitskaya, U. Mohideen, and V. M. Mostepanenko, Rev. Mod. Phys. **81**, 1827 (2009).
- [46] *Handbook of Optical Constants of Solids*, vol II, ed. E. D. Palik (Academic, New York, 1991).
- [47] L. Bergström, Adv. Colloid Interface Sci. **70**, 125 (1997).
- [48] A. Derevianko, W. R. Johnson, M. S. Safronova, and J. F. Babb, Phys. Rev. Lett. **82**, 3589 (1999).
- [49] A. Derevianko and S. G. Porsev, Phys. Rev. A **65**, 053403 (2002).
- [50] R. Brühl, P. Fouquet, R. E. Grisenti, J. P. Toennies, G. C. Hegerfeldt, T. Köhler, M. Stoll, and C. Walter, *Europhys. Lett.* **59**, 357 (2002).
- [51] B. Geyer, G. L. Klimchitskaya, and V. M. Mostepanenko, Phys. Rev. A **72**, 022111 (2005).

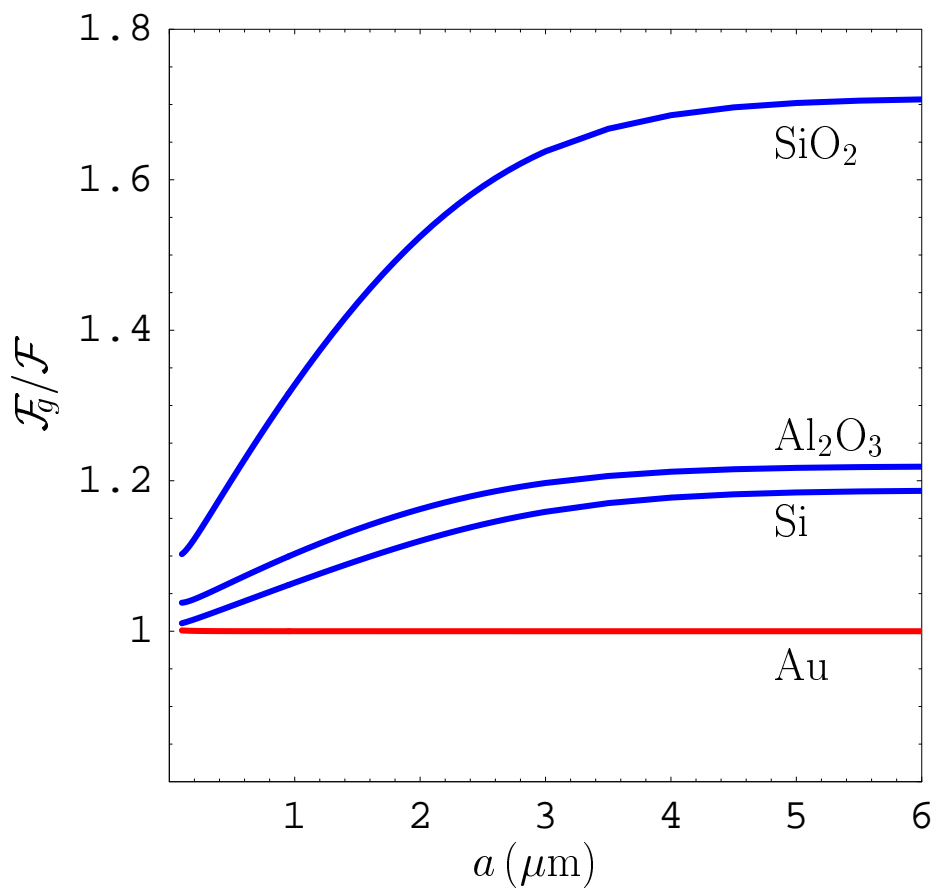


FIG. 1: (Color online) The ratios of the free energies of Casimir-Polder interaction of a Rb atom with graphene-coated and uncoated plates made of Au, Si, Al_2O_3 , and SiO_2 are shown by the four solid lines as functions of separation at $T = 300$ K.

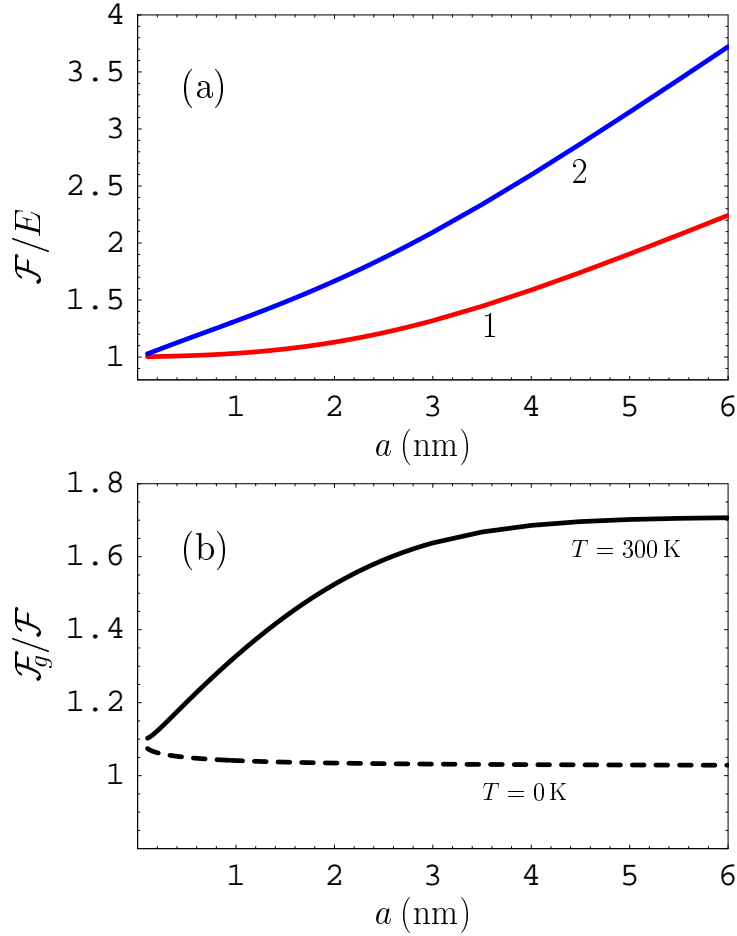


FIG. 2: (Color online) (a) The ratios of the free energy at $T = 300\text{ K}$ to the energy at $T = 0\text{ K}$ for a Rb atom interacting with an uncoated (the line 1) and graphene-coated (the line 2) SiO_2 plates are shown as functions of separation. (b) The ratios of the free energies of a Rb atom interacting with graphene-coated and uncoated SiO_2 plates as functions of separation at $T = 300\text{ K}$ (the solid line) and $T = 0\text{ K}$ (the dashed line).

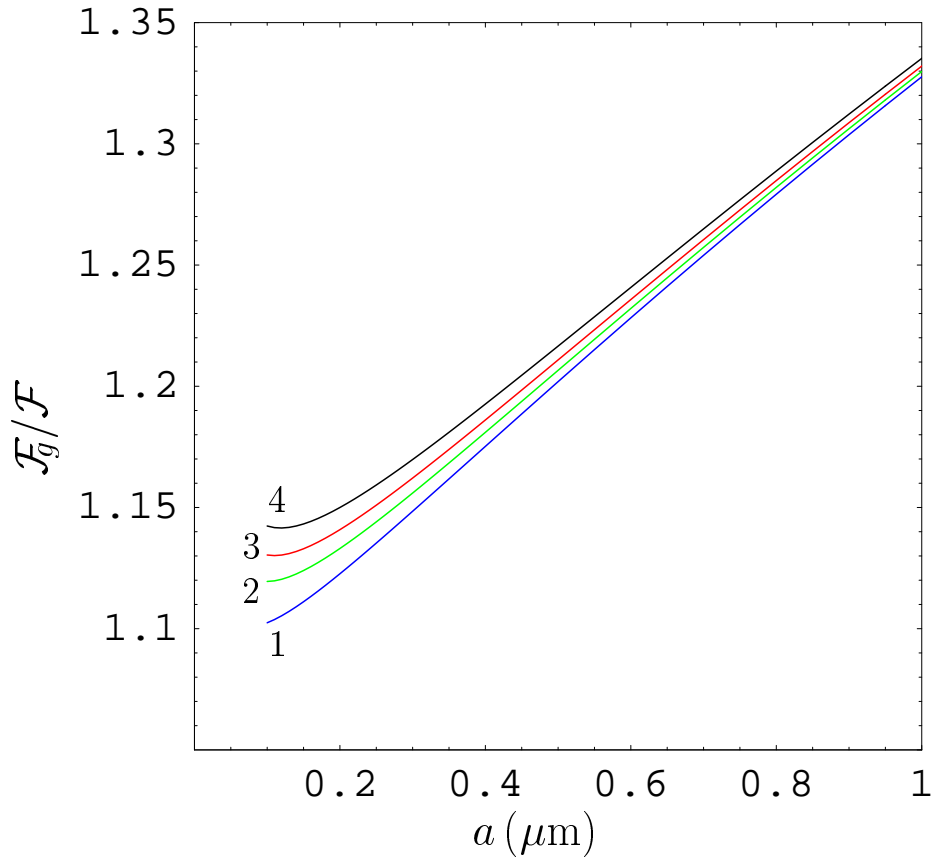


FIG. 3: (Color online) The ratios of the free energies of Casimir-Polder interaction of a Rb, Na, Cs, and He* atoms with graphene-coated and uncoated SiO₂ plates are shown at $T = 300$ K as functions of separation by the lines 1, 2, 3, and 4, respectively.

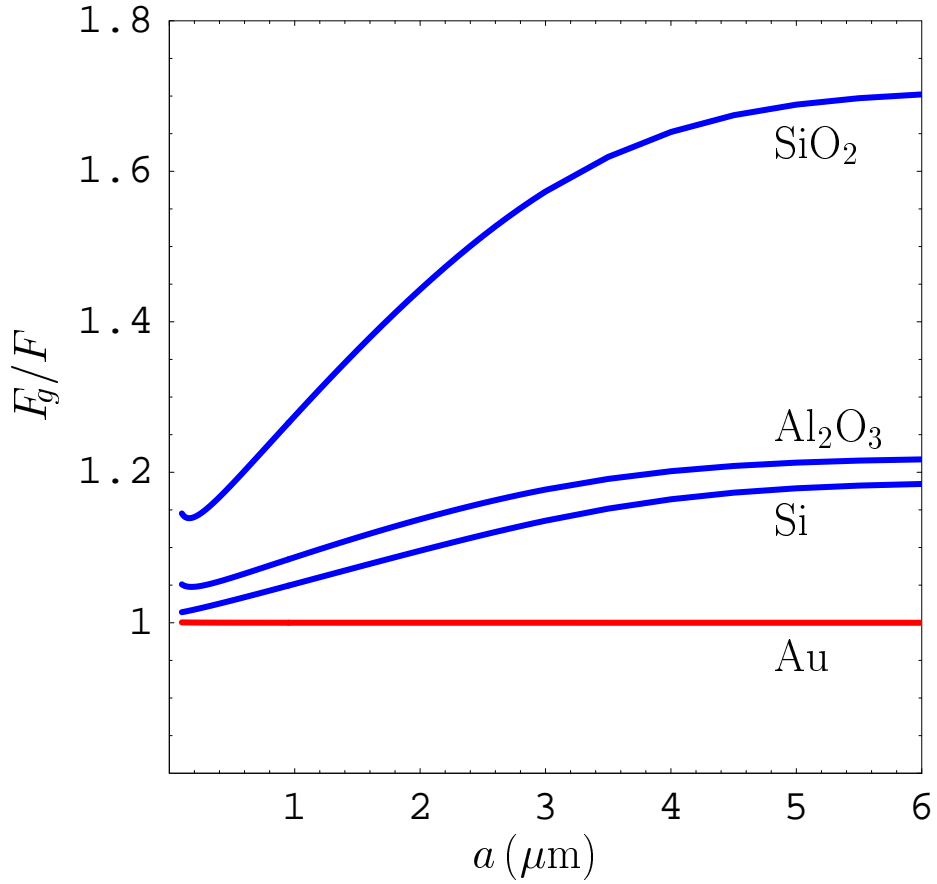


FIG. 4: (Color online) The ratios of the Casimir-Polder forces between a He^* atom and graphene-coated and uncoated plates made of Au, Si, Al_2O_3 , and SiO_2 are shown by the four solid lines as functions of separation at $T = 300$ K.

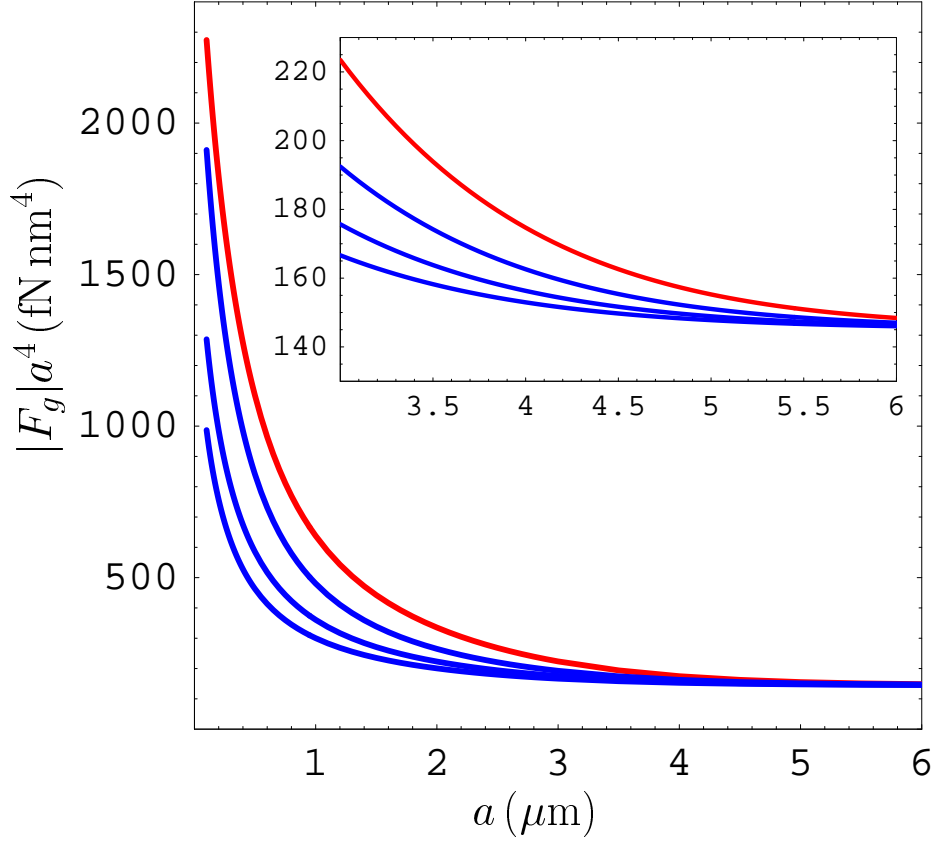


FIG. 5: (Color online) The magnitudes of the Casimir-Polder force multiplied by the fourth power of separation between an atom of He^* and graphene-coated plates made of different materials at $T = 300\text{ K}$ are shown by the four solid lines from top to bottom for the plates made of Au, Si, Al_2O_3 , and SiO_2 , respectively. The inset shows the region of large separations on an enlarged scale.

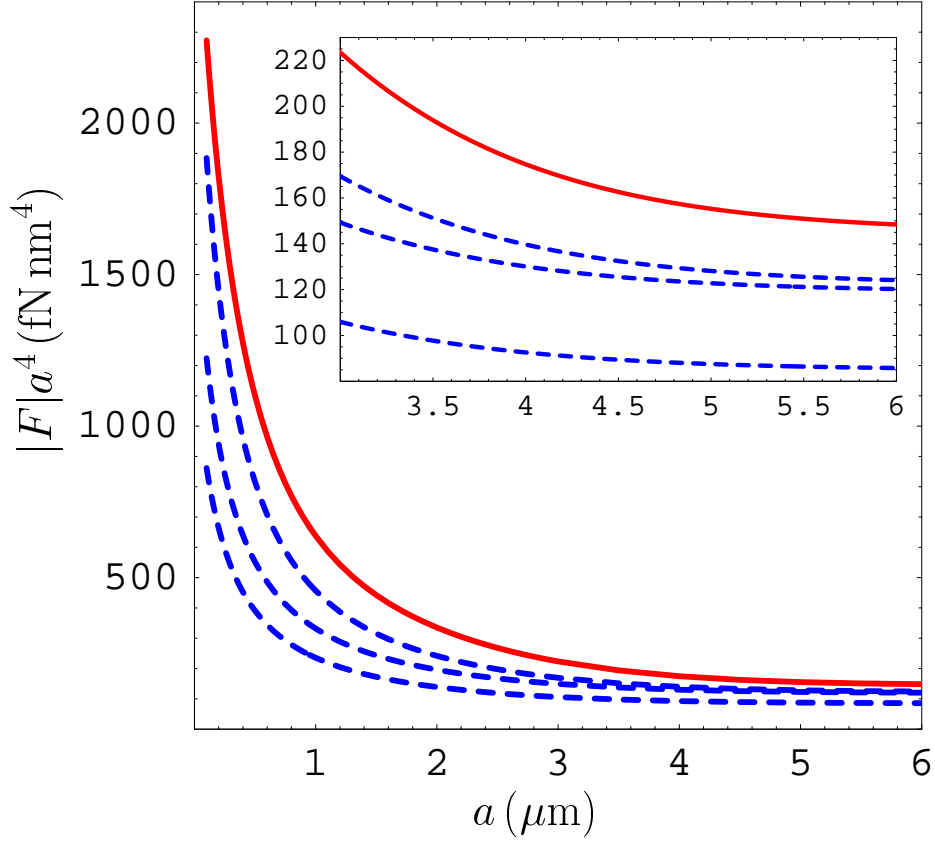


FIG. 6: (Color online) The magnitudes of the Casimir-Polder force multiplied by the fourth power of separation between an atom of He^* and uncoated plates made of different materials at $T = 300$ K are shown by the solid line for an Au plate and by the three dashed lines from top to bottom for the plates made of Si, Al_2O_3 , and SiO_2 , respectively. The inset shows the region of large separations on an enlarged scale.